Measurement of Ξ_{cc}^{++} production in *pp* collisions at $\sqrt{s}$ = 13 TeV[*]

LHCb Collaboration

R. Aaij[31]   C. Abellán Beteta[49]   T. Ackernley[59]   B. Adeva[45]   M. Adinolfi[53]   H. Afsharnia[9]   C.A. Aidala[80]

S. Aiola[25]   Z. Ajaltouni[9]   S. Akar[66]   P. Albicocco[22]   J. Albrecht[14]   F. Alessio[47]   M. Alexander[58]

A. Alfonso Albero[44]   G. Alkhazov[37]   P. Alvarez Cartelle[60]   A.A. Alves Jr[45]   S. Amato[2]   Y. Amhis[11]   L. An[21]

L. Anderlini[21]   G. Andreassi[48]   M. Andreotti[20]   F. Archilli[16]   A. Artamonov[43]   M. Artuso[67]   K. Arzymatov[41]

E. Aslanides[10]   M. Atzeni[49]   B. Audurier[26]   S. Bachmann[16]   J.J. Back[55]   S. Baker[60]   V. Balagura[11,b]

W. Baldini[20,47]   A. Baranov[41]   R.J. Barlow[61]   S. Barsuk[11]   W. Barter[60]   M. Bartolini[23,47,h]   F. Baryshnikov[77]

J.M. Basels[13]   G. Bassi[28]   V. Batozskaya[35]   B. Batsukh[67]   A. Battig[14]   A. Bay[48]   M. Becker[14]   F. Bedeschi[28]

I. Bediaga[1]   A. Beiter[67]   L.J. Bel[31]   V. Belavin[41]   S. Belin[26]   V. Bellee[48]   K. Belous[43]   I. Belyaev[38]

G. Bencivenni[22]   E. Ben-Haim[12]   S. Benson[31]   S. Beranek[13]   A. Berezhnoy[39]   R. Bernet[49]   D. Berninghoff[16]

H.C. Bernstein[67]   C. Bertella[47]   E. Bertholet[12]   A. Bertolin[27]   C. Betancourt[49]   F. Betti[19,e]   M.O. Bettler[54]

Ia. Bezshyiko[49]   S. Bhasin[53]   J. Bhom[33]   M.S. Bieker[14]   S. Bifani[52]   P. Billoir[12]   A. Bizzeti[21,u]   M. Bjørn[62]

M.P. Blago[47]   T. Blake[55]   F. Blanc[48]   S. Blusk[67]   D. Bobulska[58]   V. Bocci[30]   O. Boente Garcia[45]   T. Boettcher[63]

A. Boldyrev[78]   A. Bondar[42,x]   N. Bondar[37]   S. Borghi[61,47]   M. Borisyak[41]   M. Borsato[16]   J.T. Borsuk[33]

T.J.V. Bowcock[59]   C. Bozzi[20]   M.J. Bradley[60]   S. Braun[16]   A. Brea Rodriguez[45]   M. Brodski[47]   J. Brodzicka[33]

A. Brossa Gonzalo[55]   D. Brundu[26]   E. Buchanan[53]   A. Buonaura[49]   C. Burr[47]   A. Bursche[26]   A. Butkevich[40]

J.S. Butter[31]   J. Buytaert[47]   W. Byczynski[47]   S. Cadeddu[26]   H. Cai[72]   R. Calabrese[20,g]   L. Calero Diaz[22]   S. Cali[22]

R. Calladine[52]   M. Calvi[24,i]   M. Calvo Gomez[44,m]   P. Camargo Magalhaes[53]   A. Camboni[44,m]   P. Campana[22]

D.H. Campora Perez[31]   A.F. Campoverde Quezada[5]   L. Capriotti[19,e]   A. Carbone[19,e]   G. Carboni[29]   R. Cardinale[23,h]

A. Cardini[26]   I. Carli[6]   P. Carniti[24,i]   K. Carvalho Akiba[31]   A. Casais Vidal[45]   G. Casse[59]   M. Cattaneo[47]

G. Cavallero[47]   S. Celani[48]   R. Cenci[28,p]   J. Cerasoli[10]   M.G. Chapman[53]   M. Charles[12,47]   Ph. Charpentier[47]

G. Chatzikonstantinidis[52]   M. Chefdeville[8]   V. Chekalina[41]   C. Chen[3]   S. Chen[26]   A. Chernov[33]   S.-G. Chitic[47]

V. Chobanova[45]   S. Cholak[48]   M. Chrzaszcz[33]   A. Chubykin[37]   P. Ciambrone[22]   M.F. Cicala[55]   X. Cid Vidal[45]

G. Ciezarek[47]   F. Cindolo[19]   P.E.L. Clarke[57]   M. Clemencic[47]   H.V. Cliff[54]   J. Closier[47]   J.L. Cobbledick[61]

V. Coco[47]   J.A.B. Coelho[11]   J. Cogan[10]   E. Cogneras[9]   L. Cojocariu[36]   P. Collins[47]   T. Colombo[47]

A. Comerma-Montells[16]   A. Contu[26]   N. Cooke[52]   G. Coombs[58]   S. Coquereau[44]   G. Corti[47]   C.M. Costa Sobral[55]

B. Couturier[47]   D.C. Craik[63]   J. Crkovska[66]   A. Crocombe[55]   M. Cruz Torres[1,ab]   R. Currie[57]   C.L. Da Silva[66]

E. Dall'Occo[14]   J. Dalseno[45,53]   C. D'Ambrosio[47]   A. Danilina[38]   P. d'Argent[47]   A. Davis[61]

O. De Aguiar Francisco[47]   K. De Bruyn[47]   S. De Capua[61]   M. De Cian[48]   J.M. De Miranda[1]   L. De Paula[2]

M. De Serio[18,d]   P. De Simone[22]   J.A. de Vries[31]   C.T. Dean[66]   W. Dean[80]   D. Decamp[8]   L. Del Buono[12]

B. Delaney[54]   H.-P. Dembinski[15]   A. Dendek[34]   V. Denysenko[49]   D. Derkach[78]   O. Deschamps[9]   F. Desse[11]

F. Dettori[26]   B. Dey[7]   A. Di Canto[47]   P. Di Nezza[22]   S. Didenko[77]   H. Dijkstra[47]   V. Dobishuk[51]   F. Dordei[26]

M. Dorigo[28,y]   A.C. dos Reis[1]   L. Douglas[58]   A. Dovbnya[50]   K. Dreimanis[59]   M.W. Dudek[33]   L. Dufour[47]

G. Dujany[12]   P. Durante[47]   J.M. Durham[66]   D. Dutta[61]   M. Dziewiecki[16]   A. Dziurda[33]   A. Dzyuba[37]   S. Easo[56]

U. Egede[69]   V. Egorychev[38]   S. Eidelman[42,x]   S. Eisenhardt[57]   R. Ekelhof[14]   S. Ek-In[48]   L. Eklund[58]   S. Ely[67]

A. Ene[36]   E. Epple[66]   S. Escher[13]   S. Esen[31]   T. Evans[47]   A. Falabella[19]   J. Fan[3]   N. Farley[52]   S. Farry[59]

D. Fazzini[11]   P. Fedin[38]   M. Féo[47]   P. Fernandez Declara[47]   A. Fernandez Prieto[45]   F. Ferrari[19,e]   L. Ferreira Lopes[48]

F. Ferreira Rodrigues[2]   S. Ferreres Sole[31]   M. Ferrillo[49]   M. Ferro-Luzzi[47]   S. Filippov[40]   R.A. Fini[18]

M. Fiorini[20,g]   M. Firlej[34]   K.M. Fischer[62]   C. Fitzpatrick[47]   T. Fiutowski[34]   F. Fleuret[11,b]   M. Fontana[47]

F. Fontanelli[23,h]   R. Forty[47]   V. Franco Lima[59]   M. Franco Sevilla[65]   M. Frank[47]   C. Frei[47]   D.A. Friday[58]   J. Fu[25,q]

M. Fuehring[14]   W. Funk[47]   E. Gabriel[57]   A. Gallas Torreira[45]   D. Galli[19,e]   S. Gallorini[27]   S. Gambetta[57]

Y. Gan[3]   M. Gandelman[2]   P. Gandini[25]   Y. Gao[4]   L.M. Garcia Martin[46]   J. García Pardiñas[49]   B. Garcia Plana[45]

F.A. Garcia Rosales[11]   L. Garrido[44]   D. Gascon[44]   C. Gaspar[47]   D. Gerick[16]   E. Gersabeck[61]   M. Gersabeck[61]

T. Gershon[55]   D. Gerstel[10]   Ph. Ghez[8]   V. Gibson[54]   A. Gioventù[45]   O.G. Girard[48]   P. Gironella Gironell[44]

L. Giubega[36]   C. Giugliano[20]   K. Gizdov[57]   V.V. Gligorov[12]   C. Göbel[70]   D. Golubkov[38]   A. Golutvin[60,77]

A. Gomes[1,a]   P. Gorbounov[38,6]   I.V. Gorelov[39]   C. Gotti[24,i]   E. Govorkova[31]   J.P. Grabowski[16]   R. Graciani Diaz[44]

T. Grammatico[12]   L.A. Granado Cardoso[47]   E. Graugés[44]   E. Graverini[48]   G. Graziani[21]   A. Grecu[36]   R. Greim[31]

P. Griffith[20]   L. Grillo[61]   L. Gruber[47]   B.R. Gruberg Cazon[62]   C. Gu[3]   E. Gushchin[40]   A. Guth[13]   Yu. Guz[43,47]

T. Gys[47]   P. A. Günther[16]   T. Hadavizadeh[62]   G. Haefeli[48]   C. Haen[47]   S.C. Haines[54]   P.M. Hamilton[65]   Q. Han[7]

X. Han[16]   T.H. Hancock[62]   S. Hansmann-Menzemer[16]   N. Harnew[62]   T. Harrison[59]   R. Hart[31]   C. Hasse[14]

M. Hatch[47]   J. He[5]   M. Hecker[60]   K. Heijhoff[31]   K. Heinicke[14]   A.M. Hennequin[47]   K. Hennessy[59]   L. Henry[46]

J. Heuel[13]   A. Hicheur[68]   D. Hill[62]   M. Hilton[61]   P.H. Hopchev[48]   J. Hu[16]   W. Hu[7]   W. Huang[5]   W. Hulsbergen[31]

T. Humair[60]   R.J. Hunter[55]   M. Hushchyn[78]   D. Hutchcroft[59]   D. Hynds[31]   P. Ibis[14]   M. Idzik[34]   P. Ilten[52]

A. Inglessi[37]   K. Ivshin[37]   R. Jacobsson[47]   S. Jakobsen[47]   E. Jans[31]   B.K. Jashal[46]   A. Jawahery[65]   V. Jevtic[14]

F. Jiang[3]   M. John[62]   D. Johnson[47]   C.R. Jones[54]   B. Jost[47]   N. Jurik[62]   S. Kandybei[50]   M. Karacson[47]

J.M. Kariuki[53]   N. Kazeev[78]   M. Kecke[16]   F. Keizer[54,47]   M. Kelsey[67]   M. Kenzie[55]   T. Ketel[32]   B. Khanji[47]

A. Kharisova[79]   K.E. Kim[67]   T. Kirn[13]   V.S. Kirsebom[48]   S. Klaver[22]   K. Klimaszewski[35]   S. Koliiev[51]

A. Kondybayeva[77]   A. Konoplyannikov[38]   P. Kopciewicz[34]   R. Kopecna[16]   P. Koppenburg[31]   I. Kostiuk[31,51]

O. Kot[51]   S. Kotriakhova[37]   L. Kravchuk[40]   R.D. Krawczyk[47]   M. Kreps[55]   F. Kress[60]   S. Kretzschmar[13]

P. Krokovny[42,x]   W. Krupa[34]   W. Krzemien[35]   W. Kucewicz[33,l]   M. Kucharczyk[33]   V. Kudryavtsev[42,x]

H.S. Kuindersma[31]   G.J. Kunde[66]   T. Kvaratskheliya[38]   D. Lacarrere[47]   G. Lafferty[61]   A. Lai[26]   D. Lancierini[49]

J.J. Lane[61]   G. Lanfranchi[22]   C. Langenbruch[13]   O. Lantwin[49]   T. Latham[55]   F. Lazzari[28,v]   C. Lazzeroni[52]

R. Le Gac[10]   R. Lefèvre[9]   A. Leflat[39]   O. Leroy[10]   T. Lesiak[33]   B. Leverington[16]   H. Li[71]   L. Li[62]   X. Li[66]

Y. Li[6]   Z. Li[67]   X. Liang[67]   R. Lindner[47]   V. Lisovskyi[14]   G. Liu[71]   X. Liu[3]   D. Loh[55]   A. Loi[26]

J. Lomba Castro[45]   I. Longstaff[58]   J.H. Lopes[2]   G. Loustau[49]   G.H. Lovell[54]   Y. Lu[6]   D. Lucchesi[27,o]

M. Lucio Martinez[31]   Y. Luo[3]   A. Lupato[27]   E. Luppi[20,g]   O. Lupton[55]   A. Lusiani[28,t]   X. Lyu[5]   S. Maccolini[19,e]

F. Machefert[11]   F. Maciuc[36]   V. Macko[48]   P. Mackowiak[14]   S. Maddrell-Mander[53]   L.R. Madhan Mohan[53]

O. Maev[37,47]   A. Maevskiy[78]   D. Maisuzenko[37]   M.W. Majewski[34]   S. Malde[62]   B. Malecki[47]   A. Malinin[76]

T. Maltsev[42,x]   H. Malygina[16]   G. Manca[26,f]   G. Mancinelli[10]   R. Manera Escalero[44]   D. Manuzzi[19,e]

D. Marangotto[25,q]   J. Maratas[9,w]   J.F. Marchand[8]   U. Marconi[19]   S. Mariani[21]   C. Marin Benito[11]   M. Marinangeli[48]

P. Marino[48]   J. Marks[16]   P.J. Marshall[59]   G. Martellotti[30]   L. Martinazzoli[47]   M. Martinelli[24,i]

D. Martinez Santos[45]   F. Martinez Vidal[46]   A. Massafferri[1]   M. Materok[13]   R. Matev[47]   A. Mathad[49]   Z. Mathe[47]

V. Matiunin[38]   C. Matteuzzi[24]   K.R. Mattioli[80]   A. Mauri[49]   E. Maurice[11,b]   M. McCann[60]   L. Mcconnell[17]

A. McNab[61]   R. McNulty[17]   J.V. Mead[59]   B. Meadows[64]   C. Meaux[10]   G. Meier[14]   N. Meinert[74]   D. Melnychuk[35]

S. Meloni[24,i]   M. Merk[31]   A. Merli[25]   M. Mikhasenko[47]   D.A. Milanes[73]   E. Millard[55]   M.-N. Minard[8]

O. Mineev[38]   L. Minzoni[20,g]   S.E. Mitchell[57]   B. Mitreska[61]   D.S. Mitzel[47]   A. Mödden[14]   A. Mogini[12]

R.D. Moise[60]   T. Mombächer[14]   I.A. Monroy[73]   S. Monteil[9]   M. Morandin[27]   G. Morello[22]   M.J. Morello[28,t]

J. Moron[34]   A.B. Morris[10]   A.G. Morris[55]   R. Mountain[67]   H. Mu[3]   F. Muheim[57]   M. Mukherjee[7]   M. Mulder[47]

D. Müller[47]   K. Müller[49]   C.H. Murphy[62]   D. Murray[61]   P. Muzzetto[26]   P. Naik[53]   T. Nakada[48]   R. Nandakumar[56]
T. Nanut[48]   I. Nasteva[2]   M. Needham[57]   N. Neri[25,q]   S. Neubert[16]   N. Neufeld[47]   R. Newcombe[60]   T.D. Nguyen[48]
C. Nguyen-Mau[48,n]   E.M. Niel[11]   S. Nieswand[13]   N. Nikitin[39]   N.S. Nolte[47]   C. Nunez[80]   A. Oblakowska-
Mucha[34]   V. Obraztsov[43]   S. Ogilvy[58]   D.P. O'Hanlon[53]   R. Oldeman[26,f]   C.J.G. Onderwater[75]   J. D. Osborn[80]
A. Ossowska[33]   J.M. Otalora Goicochea[2]   T. Ovsiannikova[38]   P. Owen[49]   A. Oyanguren[46]   P.R. Pais[48]   T. Pajero[28,t]
A. Palano[18]   M. Palutan[22]   G. Panshin[79]   A. Papanestis[56]   M. Pappagallo[57]   L.L. Pappalardo[20,g]
C. Pappenheimer[64]   W. Parker[65]   C. Parkes[61]   G. Passaleva[21,47]   A. Pastore[18]   M. Patel[60]   C. Patrignani[19,e]
A. Pearce[47]   A. Pellegrino[31]   M. Pepe Altarelli[47]   S. Perazzini[19]   D. Pereima[38]   P. Perret[9]   L. Pescatore[48]
K. Petridis[53]   A. Petrolini[23,h]   A. Petrov[76]   S. Petrucci[57]   M. Petruzzo[25,q]   B. Pietrzyk[8]   G. Pietrzyk[48]   M. Pili[62]
D. Pinci[30]   J. Pinzino[47]   F. Pisani[19]   A. Piucci[16]   V. Placinta[36]   S. Playfer[57]   J. Plews[52]   M. Plo Casasus[45]
F. Polci[12]   M. Poli Lener[22]   M. Poliakova[67]   A. Poluektov[10]   N. Polukhina[77,c]   I. Polyakov[67]   E. Polycarpo[2]
G.J. Pomery[53]   S. Ponce[47]   A. Popov[43]   D. Popov[52]   S. Poslavskii[43]   K. Prasanth[33]   L. Promberger[47]   C. Prouve[45]
V. Pugatch[51]   A. Puig Navarro[49]   H. Pullen[62]   G. Punzi[28,p]   W. Qian[5]   J. Qin[5;1)]   R. Quagliani[12]   B. Quintana[8]
N.V. Raab[17]   R.I. Rabadan Trejo[10]   B. Rachwal[34]   J.H. Rademacker[53]   M. Rama[28]   M. Ramos Pernas[45]
M.S. Rangel[2]   F. Ratnikov[41,78]   G. Raven[32]   M. Reboud[8]   F. Redi[48]   F. Reiss[12]   C. Remon Alepuz[46]   Z. Ren[3]
V. Renaudin[62]   S. Ricciardi[56]   D.S. Richards[56]   S. Richards[53]   K. Rinnert[59]   P. Robbe[11]   A. Robert[12]
A.B. Rodrigues[48]   E. Rodrigues[64]   J.A. Rodriguez Lopez[73]   M. Roehrken[47]   S. Roiser[47]   A. Rollings[62]
V. Romanovskiy[43]   M. Romero Lamas[45]   A. Romero Vidal[45]   J.D. Roth[80]   M. Rotondo[22]   M.S. Rudolph[67]   T. Ruf[47]
J. Ruiz Vidal[46]   A. Ryzhikov[78]   J. Ryzka[34]   J.J. Saborido Silva[45]   N. Sagidova[37]   N. Sahoo[55]   B. Saitta[26,f]
C. Sanchez Gras[31]   C. Sanchez Mayordomo[46]   R. Santacesaria[30]   C. Santamarina Rios[45]   M. Santimaria[22]
E. Santovetti[29,j]   G. Sarpis[61]   A. Sarti[30]   C. Satriano[30,s]   A. Satta[29]   M. Saur[5]   D. Savrina[38,39]
L.G. Scantlebury Smead[62]   S. Schael[13]   M. Schellenberg[14]   M. Schiller[58]   H. Schindler[47]   M. Schmelling[15]
T. Schmelzer[14]   B. Schmidt[47]   O. Schneider[48]   A. Schopper[47]   H.F. Schreiner[64]   M. Schubiger[31]   S. Schulte[48]
M.H. Schune[11]   R. Schwemmer[47]   B. Sciascia[22]   A. Sciubba[30,k]   S. Sellam[68]   A. Semennikov[38]   A. Sergi[52,47]
N. Serra[49]   J. Serrano[10]   L. Sestini[27]   A. Seuthe[14]   P. Seyfert[47]   D.M. Shangase[80]   M. Shapkin[43]   L. Shchutska[48]
T. Shears[59]   L. Shekhtman[42,x]   V. Shevchenko[76,77]   E. Shmanin[77]   J.D. Shupperd[67]   B.G. Siddi[20]
R. Silva Coutinho[49]   L. Silva de Oliveira[2]   G. Simi[27,o]   S. Simone[18,d]   I. Skiba[20]   N. Skidmore[16]   T. Skwarnicki[67]
M.W. Slater[52]   J.G. Smeaton[54]   A. Smetkina[38]   E. Smith[13]   I.T. Smith[57]   M. Smith[60]   A. Snoch[31]   M. Soares[19]
L. Soares Lavra[9]   M.D. Sokoloff[64]   F.J.P. Soler[58]   B. Souza De Paula[2]   B. Spaan[14]   E. Spadaro Norella[25,q]
P. Spradlin[58]   F. Stagni[47]   M. Stahl[64]   S. Stahl[47]   P. Stefko[48]   O. Steinkamp[49]   S. Stemmle[16]   O. Stenyakin[43]
M. Stepanova[37]   H. Stevens[14]   S. Stone[67]   S. Stracka[28]   M.E. Stramaglia[48]   M. Straticiuc[36]   S. Strokov[79]   J. Sun[3]
L. Sun[72]   Y. Sun[65]   P. Svihra[61]   K. Swientek[34]   A. Szabelski[35]   T. Szumlak[34]   M. Szymanski[47]   S. Taneja[61]
Z. Tang[3]   T. Tekampe[14]   F. Teubert[47]   E. Thomas[47]   K.A. Thomson[59]   M.J. Tilley[60]   V. Tisserand[9]   S. T'Jampens[8]
M. Tobin[6]   S. Tolk[47]   L. Tomassetti[20,g]   D. Tonelli[28]   D. Torres Machado[1]   D.Y. Tou[12]   E. Tournefier[8]
M. Traill[58]   M.T. Tran[48]   E. Trifonova[77]   C. Trippl[48]   A. Trisovic[54]   A. Tsaregorodtsev[10]   G. Tuci[28,47,p]   A. Tully[48]
N. Tuning[31]   A. Ukleja[35]   A. Usachov[31]   A. Ustyuzhanin[41,78]   U. Uwer[16]   A. Vagner[79]   V. Vagnoni[19]
A. Valassi[47]   G. Valenti[19]   M. van Beuzekom[31]   H. Van Hecke[66]   E. van Herwijnen[47]   C.B. Van Hulse[17]
M. van Veghel[75]   R. Vazquez Gomez[44,22]   P. Vazquez Regueiro[45]   C. Vázquez Sierra[31]   S. Vecchi[20]   J.J. Velthuis[53]
M. Veltri[21,r]   A. Venkateswaran[67]   M. Vernet[9]   M. Veronesi[31]   M. Vesterinen[55]   J.V. Viana Barbosa[47]   D. Vieira[64]
M. Vieites Diaz[48]   H. Viemann[74]   X. Vilasis-Cardona[44,m]   A. Vitkovskiy[31]   V. Volkov[39]   A. Vollhardt[49]
D. Vom Bruch[12]   A. Vorobyev[37]   V. Vorobyev[42,x]   N. Voropaev[37]   R. Waldi[74]   J. Walsh[28]   J. Wang[3]   J. Wang[72]
J. Wang[6]   M. Wang[3]   Y. Wang[7]   Z. Wang[49]   D.R. Ward[54]   H.M. Wark[59]   N.K. Watson[52]   D. Websdale[60]
A. Weiden[49]   C. Weisser[63]   B.D.C. Westhenry[53]   D.J. White[61]   M. Whitehead[13]   D. Wiedner[14]   G. Wilkinson[62]
M. Wilkinson[67]   I. Williams[54]   M. Williams[63]   M.R.J. Williams[61]   T. Williams[52]   F.F. Wilson[56]   W. Wislicki[35]
M. Witek[33]   L. Witola[16]   G. Wormser[11]   S.A. Wotton[54]   H. Wu[67]   K. Wyllie[47]   Z. Xiang[5]   D. Xiao[7]   Y. Xie[7]
H. Xing[71]   A. Xu[4]   L. Xu[3]   M. Xu[7]   Q. Xu[5]   Z. Xu[4]   Z. Yang[3]   Z. Yang[65]   Y. Yao[67]   L.E. Yeomans[59]

H. Yin[7]   J. Yu[7,aa]   X. Yuan[67]   O. Yushchenko[43]   K.A. Zarebski[52]   M. Zavertyaev[15,c]   M. Zdybal[33]   M. Zeng[3]

D. Zhang[7]   L. Zhang[3]   S. Zhang[4]   W.C. Zhang[3,z]   Y. Zhang[47]   A. Zhelezov[16]   Y. Zheng[5]   X. Zhou[5]   Y. Zhou[5]

X. Zhu[3]   V. Zhukov[13,39]   J.B. Zonneveld[57]   S. Zucchelli[19,e]

[1]Centro Brasileiro de Pesquisas Físicas (CBPF), Rio de Janeiro, Brazil
[2]Universidade Federal do Rio de Janeiro (UFRJ), Rio de Janeiro, Brazil
[3]Center for High Energy Physics, Tsinghua University, Beijing, China
[4]School of Physics State Key Laboratory of Nuclear Physics and Technology, Peking University, Beijing, China
[5]University of Chinese Academy of Sciences, Beijing, China
[6]Institute Of High Energy Physics (IHEP), Beijing, China
[7]Institute of Particle Physics, Central China Normal University, Wuhan, Hubei, China
[8]Univ. Grenoble Alpes, Univ. Savoie Mont Blanc, CNRS, IN2P3-LAPP, Annecy, France
[9]Université Clermont Auvergne, CNRS/IN2P3, LPC, Clermont-Ferrand, France
[10]Aix Marseille Univ, CNRS/IN2P3, CPPM, Marseille, France
[11]LAL, Univ. Paris-Sud, CNRS/IN2P3, Université Paris-Saclay, Orsay, France
[12]LPNHE, Sorbonne Université, Paris Diderot Sorbonne Paris Cité, CNRS/IN2P3, Paris, France
[13]I. Physikalisches Institut, RWTH Aachen University, Aachen, Germany
[14]Fakultät Physik, Technische Universität Dortmund, Dortmund, Germany
[15]Max-Planck-Institut für Kernphysik (MPIK), Heidelberg, Germany
[16]Physikalisches Institut, Ruprecht-Karls-Universität Heidelberg, Heidelberg, Germany
[17]School of Physics, University College Dublin, Dublin, Ireland
[18]INFN Sezione di Bari, Bari, Italy
[19]INFN Sezione di Bologna, Bologna, Italy
[20]INFN Sezione di Ferrara, Ferrara, Italy
[21]INFN Sezione di Firenze, Firenze, Italy
[22]INFN Laboratori Nazionali di Frascati, Frascati, Italy
[23]INFN Sezione di Genova, Genova, Italy
[24]INFN Sezione di Milano-Bicocca, Milano, Italy
[25]INFN Sezione di Milano, Milano, Italy
[26]INFN Sezione di Cagliari, Monserrato, Italy
[27]INFN Sezione di Padova, Padova, Italy
[28]INFN Sezione di Pisa, Pisa, Italy
[29]INFN Sezione di Roma Tor Vergata, Roma, Italy
[30]INFN Sezione di Roma La Sapienza, Roma, Italy
[31]Nikhef National Institute for Subatomic Physics, Amsterdam, Netherlands
[32]Nikhef National Institute for Subatomic Physics and VU University Amsterdam, Amsterdam, Netherlands
[33]Henryk Niewodniczanski Institute of Nuclear Physics Polish Academy of Sciences, Kraków, Poland
[34]AGH - University of Science and Technology, Faculty of Physics and Applied Computer Science, Kraków, Poland
[35]National Center for Nuclear Research (NCBJ), Warsaw, Poland
[36]Horia Hulubei National Institute of Physics and Nuclear Engineering, Bucharest-Magurele, Romania
[37]Petersburg Nuclear Physics Institute NRC Kurchatov Institute (PNPI NRC KI), Gatchina, Russia
[38]Institute of Theoretical and Experimental Physics NRC Kurchatov Institute (ITEP NRC KI), Moscow, Russia, Moscow, Russia
[39]Institute of Nuclear Physics, Moscow State University (SINP MSU), Moscow, Russia
[40]Institute for Nuclear Research of the Russian Academy of Sciences (INR RAS), Moscow, Russia
[41]Yandex School of Data Analysis, Moscow, Russia
[42]Budker Institute of Nuclear Physics (SB RAS), Novosibirsk, Russia
[43]Institute for High Energy Physics NRC Kurchatov Institute (IHEP NRC KI), Protvino, Russia, Protvino, Russia
[44]ICCUB, Universitat de Barcelona, Barcelona, Spain
[45]Instituto Galego de Física de Altas Enerxías (IGFAE), Universidade de Santiago de Compostela, Santiago de Compostela, Spain
[46]Instituto de Fisica Corpuscular, Centro Mixto Universidad de Valencia - CSIC, Valencia, Spain
[47]European Organization for Nuclear Research (CERN), Geneva, Switzerland
[48]Institute of Physics, Ecole Polytechnique Fédérale de Lausanne (EPFL), Lausanne, Switzerland
[49]Physik-Institut, Universität Zürich, Zürich, Switzerland
[50]NSC Kharkiv Institute of Physics and Technology (NSC KIPT), Kharkiv, Ukraine
[51]Institute for Nuclear Research of the National Academy of Sciences (KINR), Kyiv, Ukraine
[52]University of Birmingham, Birmingham, United Kingdom
[53]H.H. Wills Physics Laboratory, University of Bristol, Bristol, United Kingdom
[54]Cavendish Laboratory, University of Cambridge, Cambridge, United Kingdom
[55]Department of Physics, University of Warwick, Coventry, United Kingdom
[56]STFC Rutherford Appleton Laboratory, Didcot, United Kingdom
[57]School of Physics and Astronomy, University of Edinburgh, Edinburgh, United Kingdom
[58]School of Physics and Astronomy, University of Glasgow, Glasgow, United Kingdom
[59]Oliver Lodge Laboratory, University of Liverpool, Liverpool, United Kingdom
[60]Imperial College London, London, United Kingdom
[61]Department of Physics and Astronomy, University of Manchester, Manchester, United Kingdom
[62]Department of Physics, University of Oxford, Oxford, United Kingdom
[63]Massachusetts Institute of Technology, Cambridge, MA, United States

[64]University of Cincinnati, Cincinnati, OH, United States
[65]University of Maryland, College Park, MD, United States
[66]Los Alamos National Laboratory (LANL), Los Alamos, United States
[67]Syracuse University, Syracuse, NY, United States
[68]Laboratory of Mathematical and Subatomic Physics , Constantine, Algeria, associated to [2]
[69]School of Physics and Astronomy, Monash University, Melbourne, Australia, associated to [55]
[70]Pontifícia Universidade Católica do Rio de Janeiro (PUC-Rio), Rio de Janeiro, Brazil, associated to [2]
[71]South China Normal University, Guangzhou, China, associated to [3]
[72]School of Physics and Technology, Wuhan University, Wuhan, China, associated to [3]
[73]Departamento de Fisica , Universidad Nacional de Colombia, Bogota, Colombia, associated to [12]
[74]Institut für Physik, Universität Rostock, Rostock, Germany, associated to [16]
[75]Van Swinderen Institute, University of Groningen, Groningen, Netherlands, associated to [31]
[76]National Research Centre Kurchatov Institute, Moscow, Russia, associated to [38]
[77]National University of Science and Technology "MISIS", Moscow, Russia, associated to [38]
[78]National Research University Higher School of Economics, Moscow, Russia, associated to [41]
[79]National Research Tomsk Polytechnic University, Tomsk, Russia, associated to [38]
[80]University of Michigan, Ann Arbor, United States, associated to [67]
[a]Universidade Federal do Triôngulo Mineiro (UFTM), Uberaba-MG, Brazil
[b]Laboratoire Leprince-Ringuet, Palaiseau, France
[c]P.N. Lebedev Physical Institute, Russian Academy of Science (LPI RAS), Moscow, Russia
[d]Università di Bari, Bari, Italy
[e]Università di Bologna, Bologna, Italy
[f]Università di Cagliari, Cagliari, Italy
[g]Università di Ferrara, Ferrara, Italy
[h]Università di Genova, Genova, Italy
[i]Università di Milano Bicocca, Milano, Italy
[j]Università di Roma Tor Vergata, Roma, Italy
[k]Università di Roma La Sapienza, Roma, Italy
[l]AGH - University of Science and Technology, Faculty of Computer Science, Electronics and Telecommunications, Kraków, Poland
[m]DS4DS, La Salle, Universitat Ramon Llull, Barcelona, Spain
[n]Hanoi University of Science, Hanoi, Vietnam
[o]Università di Padova, Padova, Italy
[p]Università di Pisa, Pisa, Italy
[q]Università degli Studi di Milano, Milano, Italy
[r]Università di Urbino, Urbino, Italy
[s]Università della Basilicata, Potenza, Italy
[t]Scuola Normale Superiore, Pisa, Italy
[u]Università di Modena e Reggio Emilia, Modena, Italy
[v]Università di Siena, Siena, Italy
[w]MSU - Iligan Institute of Technology (MSU-IIT), Iligan, Philippines
[x]Novosibirsk State University, Novosibirsk, Russia
[y]INFN Sezione di Trieste, Trieste, Italy
[z]School of Physics and Information Technology, Shaanxi Normal University (SNNU), Xi'an, China
[aa]Physics and Micro Electronic College, Hunan University, Changsha City, China
[ab]Universidad Nacional Autonoma de Honduras, Tegucigalpa, Honduras

Abstract: The production of Ξ_{cc}^{++} baryons in proton-proton collisions at a centre-of-mass energy of $\sqrt{s} = 13$ TeV is measured in the transverse-momentum range $4 < p_T < 15$ GeV/c and the rapidity range $2.0 < y < 4.5$. The data used in this measurement correspond to an integrated luminosity of 1.7 fb^{-1}, recorded by the LHCb experiment during 2016. The ratio of the Ξ_{cc}^{++} production cross-section times the branching fraction of the $\Xi_{cc}^{++} \to \Lambda_c^+ K^- \pi^+ \pi^+$ decay relative to the prompt Λ_c^+ production cross-section is found to be $(2.22 \pm 0.27 \pm 0.29) \times 10^{-4}$, assuming the central value of the measured Ξ_{cc}^{++} lifetime, where the first uncertainty is statistical and the second systematic.

1   Introduction

The quark model [1,2] predicts the existence of multiplets of baryon and meson states. Baryons containing two charm quarks and a light quark provide a unique system for testing the low-energy limit of quantum chromodynamics (QCD). The production of doubly charmed baryons at hadron colliders can be treated as two independent processes: production of a cc diquark followed by the

hadronisation of the diquark into a baryon [3-9]. The production cross-section of doubly charmed baryons in proton-proton collisions at a centre-of-mass energy $\sqrt{s}$ = 13 TeV is predicted to be in the range 60–1800 nb [3-9], which is between 10^{-4} and 10^{-3} times that of the total charm production [4].

A doubly charmed baryon was first reported by the SELEX collaboration [10,11]. They found that 20% of their Λ_c^+ yield originated from Ξ_{cc}^+ decays, which is several orders of magnitude higher than theoretical prediction [4]. However, this signal has not been confirmed by searches performed at the FOCUS [12], BaBar [13], Belle [14], and LHCb [15,16] experiments. Recently, the LHCb collaboration observed a peak in the $\Lambda_c^+ K^- \pi^+ \pi^+$ mass spectrum at a mass of 3621.40 ± 0.78 MeV/c^2 [17], consistent with expectations for the Ξ_{cc}^{++} baryon. The Ξ_{cc}^{++} lifetime was measured to be $0.256^{+0.024}_{-0.022}$ (stat) ± 0.014 (syst) ps [18], indicating that it decays through the weak interaction. A new decay mode, $\Xi_{cc}^{++} \to \Xi_c^+ \pi^+$, was observed by the LHCb collaboration [19], and the measured Ξ_{cc}^{++} mass was found to be consistent with that measured using $\Xi_{cc}^{++} \to \Lambda_c^+ K^- \pi^+ \pi^+$ decays. The $\Xi_{cc}^{++} \to D^+ p K^- \pi^+$ decay has been searched for, but no signal was found [20].

This paper presents a measurement of Ξ_{cc}^{++} production in pp collisions at a centre-of-mass energy of $\sqrt{s}$ = 13 TeV, following the same analysis strategy as that used in Refs. [15,17,18]. The Ξ_{cc}^{++} production cross-section, $\sigma(\Xi_{cc}^{++})$, times the branching fraction of the $\Xi_{cc}^{++} \to \Lambda_c^+ K^- \pi^+ \pi^+$ decay, is measured relative to the prompt Λ_c^+ production cross-section, $\sigma(\Lambda_c^+)$, in the transverse momentum range $4 < p_T < 15$ GeV/c and the rapidity range $2.0 < y < 4.5$. The data used correspond to an integrated luminosity of 1.7 fb^{-1} collected by the LHCb experiment in 2016. The Λ_c^+ baryon is reconstructed via the $\Lambda_c^+ \to p K^- \pi^+$ decay. The inclusion of the charge-conjugate decay processes is implied throughout this paper. The production rate ratio is defined as,

$$R \equiv \frac{\sigma(\Xi_{cc}^{++}) \times \mathcal{B}(\Xi_{cc}^{++} \to \Lambda_c^+ K^- \pi^+ \pi^+)}{\sigma(\Lambda_c^+)} = \frac{N_{sig}}{N_{norm}} \frac{\varepsilon_{norm}}{\varepsilon_{sig}}, \quad (1)$$

where "sig" and "norm" refer to the signal (Ξ_{cc}^{++}) and normalisation (Λ_c^+) modes, N is the signal yield and ε is the total efficiency to reconstruct and select these decays.

2   Detector and simulation

The LHCb detector [21,22] is a single-arm forward spectrometer covering the pseudorapidity range $2 < \eta < 5$, designed for the study of particles containing b or c quarks. The detector includes a high-precision tracking system consisting of a silicon-strip vertex detector surrounding the pp interaction region [23], a large-area silicon-strip detector located upstream of a dipole magnet

with a bending power of about 4 Tm, and three stations of silicon-strip detectors and straw drift tubes [24] placed downstream of the magnet. The tracking system provides a measurement of the momentum, p, of charged particles with a relative uncertainty that varies from 0.5% at low momentum to 1.0% at 200 GeV/c. The minimum distance of a track to a primary vertex, the impact parameter, is measured with a resolution of $(15 + 29/p_T)$ μm, where p_T is expressed in GeV/c. Different types of charged hadrons are distinguished using information from two ring-imaging Cherenkov detectors [25]. Photons, electrons and hadrons are identified by a calorimeter system consisting of scintillating-pad (SPD) and preshower detectors, an electromagnetic and a hadronic calorimeter. Muons are identified by a system composed of alternating layers of iron and multiwire proportional chambers [26]. The online event selection is performed by a trigger [27], which consists of a hardware stage, based on information from the calorimeters and muon systems [28,29], followed by a software stage, which applies a full event reconstruction incorporating near-real-time alignment and calibration of the detector [30]. The output of the reconstruction performed in the software trigger [31] is used as input to the present analysis.

Simulated samples are required to develop the candidate selection and to estimate the efficiency of the detector acceptance and the imposed selection requirements. Simulated pp collisions are generated using PYTHIA [32] with a specific LHCb configuration [33]. A dedicated package, GENXICC2.0 [34], is used to simulate the Ξ_{cc}^{++} baryon production. Decays of unstable particles are described by EVTGEN [35], in which final-state radiation is generated using PHOTOS [36]. The interaction of the generated particles with the detector, and its response, are simulated using the GEANT4 toolkit [37] as described in Ref. [38].

3   Event selection

The $\Lambda_c^+ \to p K^- \pi^+$ candidate is reconstructed through three charged particles identified as p, K^- and π^+ hadrons, which form a common vertex and do not originate from any primary vertex (PV) in the event. The decay vertex of the Λ_c^+ candidate is required to be displaced from any PV by requiring its proper decay time to be greater than 0.15 ps, corresponding to about 1.5 times the Λ_c^+ decay time resolution [39]. Each Λ_c^+ candidate with mass in the range 2270-2306 MeV/c^2 is then combined with three additional particles to form a Ξ_{cc}^{++} candidate. The three particles must form a common vertex with the Λ_c^+ candidate and have hadron-identification information consistent with them being two π^+ mesons and one K^- meson. The Λ_c^+ decay vertex is required to be downstream of the Ξ_{cc}^{++} ver-

tex. Additionally, the $\varXi_{cc}^{++}$ candidates must have $p_{\mathrm{T}} > 4 \,\mathrm{GeV}/c$ and originate from a PV.

The combinatorial background is suppressed using two multivariate classifiers based on a boosted decision tree algorithm [40]. One classifier is optimised to select $\varLambda_c^+$ candidates irrespective of their origin, and the other is optimised to select $\varXi_{cc}^{++}$ candidates. While both classifiers are applied to the signal channel, only the first is applied to the normalisation decay channel. The first classifier is trained with $\varLambda_c^+$ signal in the simulated $\varXi_{cc}^{++}$ sample and background candidates in the $\varLambda_c^+$ mass sideband. The second classifier is trained using data candidates in the $\varLambda_c^+$ and $\varXi_{cc}^{++}$ signal mass region, where wrong-sign (WS) $\varLambda_c^+ K^- \pi^+ \pi^-$ combinations are used as proxy for the background. The first multivariate classifier is trained with the following variables: the χ^2 of the $\varLambda_c^+$ vertex fit; the largest distance of closest approach among the decay products; the scalar sum of the p_{T} and the smallest p_{T} of the three decay products of the $\varLambda_c^+$ candidate; the smallest and largest χ_{IP}^2 of the decay products of the $\varLambda_c^+$ candidate with respect to its PV. Here, χ_{IP}^2 is defined as the difference in χ^2 of the PV fit with and without the particle in question. The PV of any single particle is defined to be that with respect to which the particle has the smallest χ_{IP}^2. The second multivariate classifier is trained with the following variables: the χ_{IP}^2 of the $\varXi_{cc}^{++}$ candidate to its PV; the angle between the $\varXi_{cc}^{++}$ momentum and the direction from the PV to the $\varXi_{cc}^{++}$ decay vertex; the logarithm of the χ^2 of the $\varXi_{cc}^{++}$ flight distance between the $\varXi_{cc}^{++}$ decay vertex and the PV; the vertex fit χ^2 of the $\varXi_{cc}^{++}$ candidate; the χ^2 of a kinematic refit [41] that requires the $\varXi_{cc}^{++}$ candidate to originate from a PV; the scalar sum of the p_{T} and the smallest p_{T} of the six final state tracks of the $\varXi_{cc}^{++}$ candidate. Here the flight distance χ^2 is defined as the change in χ^2 of the $\varXi_{cc}^{++}$ decay vertex if it is constrained to coincide with the PV. Candidates retained for analysis must have two classifier responses exceeding thresholds chosen by performing a two-dimensional maximisation of the figure of merit $\varepsilon/(5/2 + \sqrt{B})$ [42]. Here ε and B are the estimated signal efficiency determined from signal simulation and background yield under the signal peak, respectively. The background is estimated from the WS sample. The same threshold of the first classifier, optimised for the signal mode, is applied to the normalisation mode.

Finally, the $\varXi_{cc}^{++}$ and $\varLambda_c^+$ candidates are required to have their transverse momentum and rapidity in the fiducial ranges of 4-15 GeV/c and 2.0-4.5, respectively. After the multivariate selection is applied, events may still contain more than one $\varXi_{cc}^{++}$ candidate in the signal region. Candidates made of duplicate tracks are removed by requiring all pairs of tracks with the same charge to have an opening angle larger than 0.5 mrad. Duplicate candidates, which are due to the interchange between identical particles from the $\varLambda_c^+$ decay or directly from the $\varXi_{cc}^{++}$ decay (e.g., the K^- particle from the $\varXi_{cc}^{++}$ decay and the K^- particle from the $\varLambda_c^+$ decay), can cause peaking structures in the $\varXi_{cc}^{++}$ invariant mass distribution. In this case, one of the candidates is chosen at random to be retained and the others are discarded. The systematic uncertainty associated with this procedure is negligible.

4   Signal yields

After the full selection is applied, the data sets are further filtered into two disjoint subsamples using information from the hardware trigger. The first contains candidates that are triggered by at least one of the $\varLambda_c^+$ decay products with high transverse energy deposited in the calorimeters, referred to as Triggered On Signal (TOS). The second consists of the events that are exclusively triggered by particles unrelated to the signal decay products; these events can, for example, be triggered by the decay products of the charmed hadrons produced together with the signal baryon, referred to as exclusively Triggered Independently of Signal (exTIS).

To determine the $\varXi_{cc}^{++}$ baryon signal yields, an unbinned extended maximum-likelihood fit is performed simultaneously to the $\varLambda_c^+ K^- \pi^+ \pi^+$ invariant-mass spectra in the interval 3470-3770 MeV/c^2 of the two trigger categories. The mass distribution of the signal is described by the sum of a Gaussian function and a modified Gaussian function with power-law tails on both sides of the function [43] with a common peak position. The tail parameters and the relative fraction of the two Gaussian functions for the signal model are determined from simulation, while the common peak position and the mass resolution are allowed to vary in the fit. The background is described by a second-order Chebyshev polynomial. Fig. 1 shows the $\varLambda_c^+ K^- \pi^+ \pi^+$ invariant-mass distribution in data together with the fit results for the two trigger categories. The fit returns a mass of $3621.34 \pm 0.74 \,\mathrm{MeV}/c^2$, and a mass resolution of $7.1 \pm 1.3 \,\mathrm{MeV}/c^2$, where the uncertainties are statistical only.

The determination of the prompt $\varLambda_c^+$ baryon yields, which are contaminated by $\varLambda_c^+$ candidates produced in b-hadron decays, is done in two steps [44]. First, a binned extended maximum-likelihood fit to the $m(pK^-\pi^+)$ invariant-mass distribution in the interval 2220-2360 MeV/c^2 is performed to determine the total number of $\varLambda_c^+$ candidates. Then a binned extended maximum-likelihood fit to the background-subtracted $\log_{10}\left(\chi_{\mathrm{IP}}^2(\varLambda_c^+)\right)$ distribution is performed to separate the prompt $\varLambda_c^+$ component from that originated in b-hadron decays. The mass distribution of $\varLambda_c^+$ candidates is described by a sum of a Gaussian function and a modified Gaussian function with power-law tails on both sides with a common peak position. The

background mass distribution is described by a first-order Chebyshev polynomial. The $\log_{10}\left(\chi^2_{\mathrm{IP}}(\Lambda_c^+)\right)$ distribution, after subtracting the combinatorial background using the *sPlot* technique [45], is described by two Bukin functions [46]. All the parameters except the peak position and resolution of the functions are derived from a fit to simulated signal. Figs. 2 and 3 show the $pK^-\pi^+$ invariant-mass distribution and $\log_{10}\left(\chi^2_{\mathrm{IP}}(\Lambda_c^+)\right)$ distributions in data together with the fit results for the two trigger categories. The signal yields for both the signal and the normalisation modes are presented in Table 1.
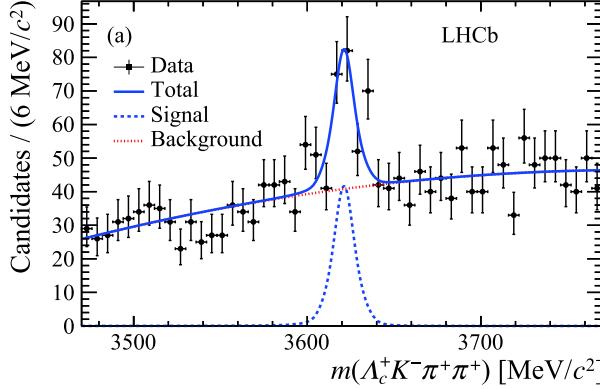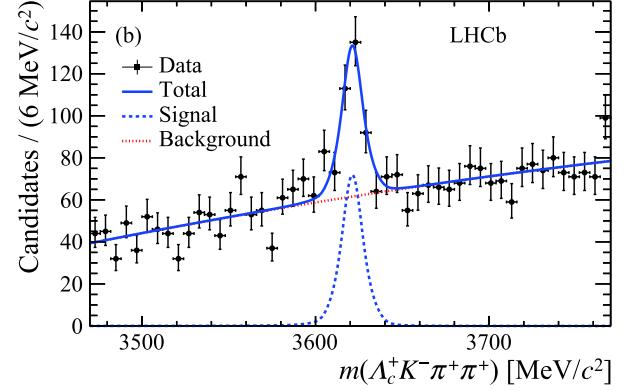
Fig. 1.   (color online) Invariant-mass distributions of Ξ_{cc}^{++} candidates (a) triggered by TOS and (b) triggered by exTIS, with fit results shown.
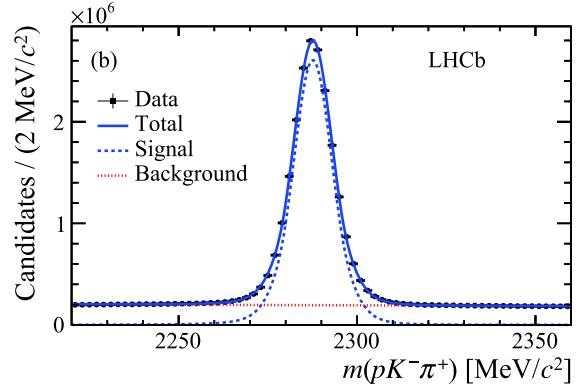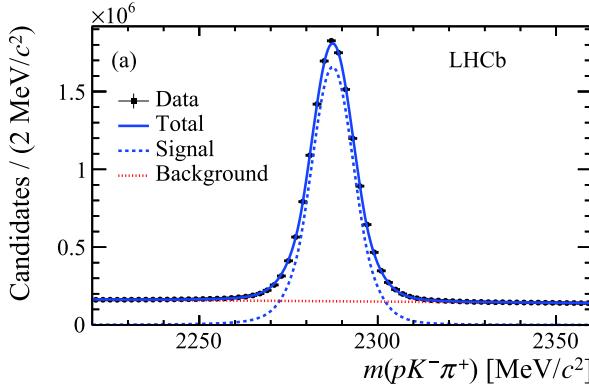
Fig. 2.   (color online) Invariant-mass distributions of Λ_c^+ candidates (a) triggered by TOS and (b) triggered by exTIS, with fit results shown.
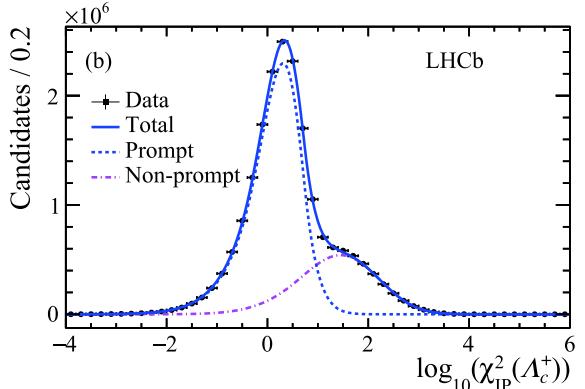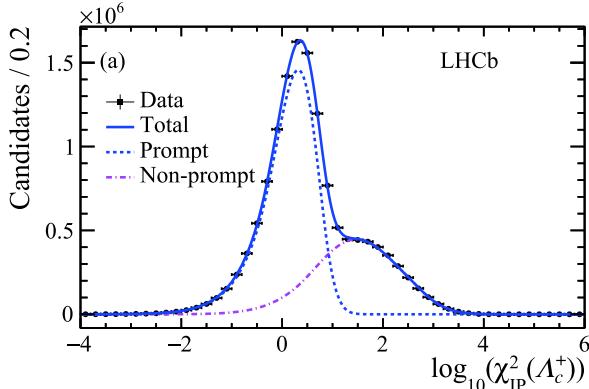

Fig. 3.   (color online) Distributions of $\log_{10}\left(\chi^2_{\mathrm{IP}}(\Lambda_c^+)\right)$ for background-subtracted candidates (a) triggered by TOS and (b) triggered by exTIS, with fit results shown.

Table 1.   Yields of the signal and normalisation modes.

Category	N_{sig}	N_{norm} [10^3]
TOS	116 ± 23	8764 ± 6
exTIS	210 ± 29	13889 ± 8

5   Efficiencies

For each trigger category and for both the signal and the normalisation channels, the total efficiencies are computed as products of the detector geometrical acceptance and of the efficiencies related to particle reconstruction, event selection, particle identification and trigger. All the efficiencies are calculated using simulation that is corrected using data. For both the signal and the normalisation modes, the kinematic distributions in simulation samples, including the transverse momentum and rapidity of the Ξ_{cc}^{++} and Λ_c^+ baryons and the event multiplicity, are weighted to match those in the corresponding data. The efficiencies are calculated under three lifetime $\left(\tau_{\Xi_{cc}^{++}}\right)$ hypotheses: the central value of the measured lifetime, and the lifetime increased or decreased by its measured uncertainty [18]. The dependence of the efficiency on the Ξ_{cc}^{++} baryon lifetime is almost linear, with the efficiency ratio varying by 25% from the lower lifetime to the higher one. The resonant structures of the $\Lambda_c^+ \to pK^-\pi^+$ decay are also weighted based on the background-subtracted data, as the simulation samples do not model well the structure seen in the data. The tracking efficiency is corrected with control data samples, as described in Ref. [47]. The particle-identification efficiency is corrected in bins of particle momentum, pseudorapidity and event multiplicity, using the results of a tag-and-probe method applied to calibration samples [48]. The efficiency ratios of the normalisation mode to the signal mode are presented in Table 2.

Table 2.   Ratios of the normalisation and signal efficiencies.

Category	$\varepsilon_{norm}/\varepsilon_{sig}$		
	$\tau_{\Xi_{cc}^{++}} = 0.230$ ps	$\tau_{\Xi_{cc}^{++}} = 0.256$ ps	$\tau_{\Xi_{cc}^{++}} = 0.284$ ps
TOS	22.00 ± 1.09	19.50 ± 1.71	17.50 ± 1.50
exTIS	16.64 ± 1.30	14.56 ± 1.06	12.95 ± 0.80

6   Systematic uncertainties

The sources of systematic uncertainties affecting the measurement of the production ratio include the choice of the fit model and the evaluation of the total efficiency. The uncertainties are summarised in Table 3.

For both the signal and normalisation modes, the uncertainties due to the choice of the particular fit model are estimated by using alternative functions where the signal

Table 3.   Relative systematic uncertainties on the production ratio measurement for the two trigger categories.

Source	TOS [%]	exTIS [%]
Simulation sample size	8.8	7.3
Fit model	5.4	5.3
Hardware trigger	9.0	6.3
Tracking	3.4	3.4
Particle identification	5.5	5.4
Kinematic correction	7.3	6.0
Sum in quadrature	16.8	14.1

is described by a sum of two Gaussian functions with a common peak position and the background is described by a second-order polynomial function. The difference in the ratio of signal yields between the two fits is assigned as systematic uncertainty. Additional effects coming from the $\log_{10}\left(\chi_{IP}^2(\Lambda_c^+)\right)$ fit are tested with alternative functions where the parameters used to describe the nonprompt signal are determined from a Λ_b^0 baryon data sample. The effect from the background subtraction is studied using the shape determined with the candidates in the Λ_c^+ baryon mass sidebands.

The limited size of the simulation samples leads to systematic uncertainties on the efficiencies. The systematic uncertainty due to the trigger selection efficiency is estimated with a tag-and-probe method exploiting a sample of events that are also triggered by particles unrelated to the signal candidate [27]. Due to the small sample size of the signal channel in data, two different control samples are used. The first sample comprises $\Lambda_b^0 \to \Lambda_c^+\pi^-\pi^+\pi^-$ decays, which are topologically similar to the $\Xi_{cc}^{++} \to \Lambda_c^+K^-\pi^+\pi^+$ decay. The second sample comprises $B_c^+ \to J/\psi\pi^+$ decays. This decay does not have the same topology but shares another feature with the signal: there should be at least two other heavy-flavour particles (b- or c-hadrons) produced in the same event that can be responsible for the trigger decision. The hardware trigger efficiencies of the Λ_b^0, B_c^+ decay channels and prompt Λ_c^+ channel, are measured using the tag-and-probe method. Similar selections to those applied to the signal channel are applied to both the data and simulation for the control samples. The efficiency ratio of the Λ_b^0, B_c^+ decays to the Λ_c^+ decays is estimated and the difference of the ratio in data and in simulation is assigned as a systematic uncertainty. The transverse-energy threshold in the calorimeter hardware trigger varied during data taking, and this variation is not fully described by the simulation. The threshold used in the simulated samples is higher than that applied to some data. To investigate the influence of this difference, the same hardware trigger requirement used in the simulation is applied to the data. The meas-

urement is repeated and the change in the measured production ratio is taken as a systematic uncertainty.

The systematic uncertainty related to the tracking efficiency includes three effects. First, the tracking efficiency depends on the detector occupancy, which is not well described by simulation. The distribution of the number of SPD hits in simulated samples is weighted to match that in data and an uncertainty of 0.8% per track is assigned to account for remaining difference in multiplicity between data and simulation [47]. Secondly, the uncertainty due to the finite size of the control samples is propagated to the final systematic uncertainty using a large number of pseudoexperiments. Finally, an uncertainty is assigned to the track reconstruction efficiency due to uncertainties on the material budget of the detector and on the modelling of hadronic interaction with the detector material.

The systematic uncertainty related to the particle-identification efficiency includes three effects. The effect from the limited size of calibration samples is evaluated with a large number of pseudoexperiments. Effects of binning in momentum, pseudorapidity and event multiplicity is evaluated by increasing or decreasing the bin sizes by a factor of two. In this estimation, the effects of the correlations between tracks on the particle identification performance are taken into account using simulated samples.

The uncertainties on the weights used for the correction of the kinematic distributions of the simulation samples are propagated as a systematic uncertainty on the production ratio.

7   Results

The production-rate ratio is calculated for the TOS and the exTIS categories of events for three different Ξ_{cc}^{++} lifetime scenarios using Eq. (1). The separate ratios in the TOS and exTIS categories are presented in Table 4 and are found to be consistent. The combination of the trig-

Table 4.   Production rate ratio results for three different Ξ_{cc}^{++} lifetime hypotheses. The first uncertainty is statistical and the second is systematic.

Category	$R\,[10^{-4}]$		
	$\tau_{\Xi_{cc}^{++}} = 0.230$ ps	$\tau_{\Xi_{cc}^{++}} = 0.256$ ps	$\tau_{\Xi_{cc}^{++}} = 0.284$ ps
TOS	$2.90 \pm 0.57 \pm 0.49$	$2.57 \pm 0.51 \pm 0.43$	$2.31 \pm 0.46 \pm 0.39$
exTIS	$2.41 \pm 0.35 \pm 0.34$	$2.11 \pm 0.31 \pm 0.30$	$1.88 \pm 0.27 \pm 0.27$
Combined	$2.53 \pm 0.30 \pm 0.33$	$2.22 \pm 0.27 \pm 0.29$	$1.98 \pm 0.23 \pm 0.26$

ger categories, using the Best Linear Unbiased Estimate method [49] is also reported. In the combination, the systematic uncertainties coming from the simulation sample size and hardware trigger are assumed to be uncorrelated, while the other systematic uncertainties are considered to be 100% correlated.

8   Conclusion

A first measurement of the Ξ_{cc}^{++} production cross-section relative to that of Λ_c^+ baryons is presented. The ratio of Ξ_{cc}^{++} production cross-section times the branching fraction of the $\Xi_{cc}^{++} \to \Lambda_c^+ K^- \pi^+ \pi^+$ decay relative to the prompt Λ_c^+ production cross-section in the kinematic region $4 < p_T < 15$ GeV/c and $2.0 < y < 4.5$ is measured to be $(2.22 \pm 0.27 \pm 0.29) \times 10^{-4}$, assuming the central value of the Ξ_{cc}^{++} lifetime measured in Ref. [18], where the first uncertainty is statistical and the second systematic. This is the first measurement of the production of the doubly charmed baryons in pp collisions and will deepen our understanding on their production mechanism.

References

1   M. Gell-Mann, Phys. Lett., 8: 214 (1964)
2   G. Zweig, Tech. Rep. CERN-TH-401, CERN, Geneva, 1964
3   A. V. Berezhnoy, V. V. Kiselev, A. K. Likhoded et al, Phys. Rev. D, 57: 4385 (1998), arXiv:hep-ph/9710339
4   V. V. Kiselev and A. K. Likhoded, Phys. Usp., 45: 455 (2002), arXiv:hep-ph/0103169
5   J. P. Ma and Z. G. Si, Phys. Lett. B, 568: 135 (2003), arXiv:hep-ph/0305079
6   C.-H. Chang, J.-P. Ma, C.-F. Qiao et al, J. Phys. G, 34: 845 (2007), arXiv:hep-ph/0610205
7   C.-H. Chang, C.-F. Qiao, J.-X. Wang et al, Phys. Rev. D, 73: 094022 (2006), arXiv:hep-ph/0601032
8   J.-W. Zhang et al, Phys. Rev. D, 83: 034026 (2011), arXiv:1101.1130
9   C.-H. Chang, C.-F. Qiao, J.-X. Wang et al, Phys. Rev. D, 71: 074012 (2005), arXiv:hep-ph/0502155
10   SELEX Collaboration, M. Mattson et al, Phys. Rev. Lett., 89: 112001 (2002), arXiv:hep-ex/0208014
11   SELEX Collaboration, A. Ocherashvili et al, Phys. Lett. B, 628: 18 (2005), arXiv:hep-ex/0406033
12   S. P. Ratti et al, Nucl. Phys. Proc. Suppl., 115: 33 (2003)
13   BaBar Collaboration, B. Aubert et al, Phys. Rev. D, 74: 011103 (2006), arXiv:hep-ex/0605075
14   Belle Collaboration, R. Chistov et al, Phys. Rev. Lett., 97: 162001 (2006), arXiv:hep-ex/0606051
15   LHCb Collaboration, R. Aaij et al, JHEP, 12: 090 (2013), arXiv:1310.2538
16   LHCb Collaboration, R. Aaij et al, Sci. China-Phys. Mech.

Astron., **63**: 221062 (2020), arXiv: 1909.12273

17 LHCb Collaboration, R. Aaij et al, Phys. Rev. Lett., **119**: 112001 (2017), arXiv:1707.01621

18 LHCb Collaboration, R. Aaij et al, Phys. Rev. Lett., **121**: 052002 (2018), arXiv:1806.02744

19 LHCb Collaboration, R. Aaij et al, Eur. Phys. J. C, **78**: 443 (2018), arXiv:1712.08609

20 LHCb Collaboration, R. Aaij et al, JHEP, **10**: 124 (2019), arXiv:1905.02421

21 LHCb Collaboration, A. A. Alves Jr. et al, JINST, **3**: S08005 (2008)

22 LHCb Collaboration, R. Aaij et al, Int. J. Mod. Phys. A, **30**: 1530022 (2015), arXiv:1412.6352

23 R. Aaij et al, JINST, **9**: P09007 (2014), arXiv:1405.7808

24 P. d'Argent et al, JINST, **12**: P11016 (2017), arXiv:1708.00819

25 M. Adinolfi et al, Eur. Phys. J. C, **73**: 2431 (2013), arXiv:1211.6759

26 A. A. Alves Jr. et al, JINST, **8**: P02022 (2013), arXiv:1211.1346

27 R. Aaij et al, JINST, **8**: P04022 (2013), arXiv:1211.3055

28 R. Aaij et al, LHCb-DP-2013-004, in preparation

29 F. Archilli et al, JINST, **8**: P10020 (2013), arXiv:1306.0249

30 R. Aaij et al, JINST, **14**: P04013 (2019), arXiv:1812.10790

31 R. Aaij et al, Comput. Phys. Commun., **208**: 35 (2016), arXiv:1604.05596

32 T. Sjöstrand, S. Mrenna, and P. Skands, Comput. Phys. Commun., **178**: 852 (2008), arXiv: 0710.3820; T. Sjöstrand, S. Mrenna, and P. Skands, JHEP **05**: 026 (2006), arXiv: hep-ph/0603175

33 I. Belyaev et al, J. Phys. Conf. Ser., **331**: 032047 (2011)

34 C.-H. Chang, J.-X. Wang, and X.-G. Wu, Comput. Phys. Commun., **181**: 1144 (2010), arXiv:0910.4462

35 D. J. Lange, Nucl. Instrum. Meth. A, **462**: 152 (2001)

36 P. Golonka and Z. Was, Eur. Phys. J. C, **45**: 97 (2006), arXiv:hep-ph/0506026

37 Geant4 Collaboration, J. Allison et al, IEEE Trans. Nucl. Sci., **53**: 270 (2006); Geant4 Collaboration, S. Agostinelli et al, Nucl. Instrum. Meth. A, **506**: 250 (2003)

38 M. Clemencic et al, J. Phys. Conf. Ser., **331**: 032023 (2011)

39 Particle Data Group, M. Tanabashi et al, Phys. Rev. D, **98**: 030001 (2018)

40 H. Voss, A. Hoecker, J. Stelzer et al, PoS **ACAT** (2007) 040; A. Hoecker et al, *TMVA 4- Toolkit for Multivariate Data Analysis with ROOT. Users Guide.*, arXiv: physics/0703039

41 W. D. Hulsbergen, Nucl. Instrum. Meth. A, **552**: 566 (2005), arXiv:physics/0503191

42 G. Punzi, eConf, **C030908**: MODT002 (2003), arXiv:physics/0308063

43 T. Skwarnicki, PhD thesis, Institute of Nuclear Physics, Krakow, 1986, DESY-F31-86-02

44 LHCb Collaboration, R. Aaij et al, Nucl. Phys. B, **871**: 1 (2013), arXiv:1302.2864

45 M. Pivk and F. R. Le Diberder, Nucl. Instrum. Meth. A, **555**: 356 (2005), arXiv:physics/0402083

46 A. D. Bukin, arXiv: 0711.4449

47 LHCb Collaboration, R. Aaij et al, JINST, **10**: P02007 (2015), arXiv:1408.1251

48 R. Aaij et al, Eur. Phys. J. Tech. Instr., **6**: 1 (2018), arXiv:1803.00824

49 R. Nisius, Eur. Phys. J. C, **74**: 3004 (2014), arXiv: 1402.4016; R. Nisius, *Blue: a software package to combine correlated estimates of physics observables within root using the best linear unbiased estimate method - program manual, version 2.1.0*, http://blue.hepforge.org.